Keeyask Generation Project

Environmental Impact Statement

Supporting Volume

Physical Environment

Hydropower Limited Partnership

June 2012

APPENDIX 6A

SHORELINE EROSION PROCESSES DESCRIPTION OF MODELS

This page is intentionally left blank.

TABLE OF CONTENTS

LIST OF TABLES

Page

LIST OF FIGURES

Page

LIST OF MAPS

Page

This page is intentionally left blank.

6A.0 DESCRIPTION OF MODELS

6A.1 PEATLAND DISINTEGRATION

6A.1.1 Model Overview

At the most basic level, the peatland disintegration model consists of a schematic representation of the post-flooding pathways (see Figure 6A.1-1 for an example) revealed by analysis of the Stephens Lake time series photography and supported by other available information.

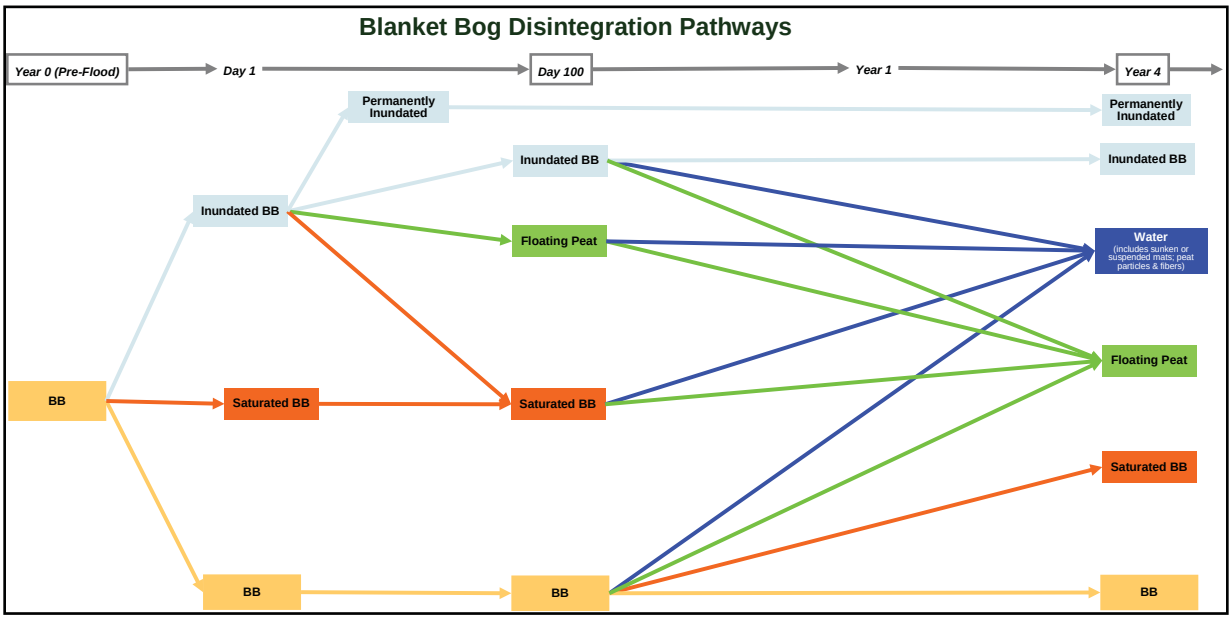

Figure 6A.1-1: Schematic Peatland Disintegration Pathway Model Derived from Proxy Area Data

Available project data, field experience and literature supported the development of a GIS-based mixed process and empirical spatial model. The model is a spatial model in the sense that it incorporates adjacency and distance relationships.

The peatland disintegration model is structured as a series of logical tests or equations arranged in a decision tree. The decision tree identifies possible states at the start of a prediction period and then applies logical tests or equations to each state to predict how much of the peatland area in that state will follow a particular pathway during the prediction period. The potential starting states and peatland disintegration pathways were derived from proxy area data. Figure 6A.1-1 shows the blanket peatland decision tree or pathway model. The first branch in the decision tree asks whether the peat patch is flooded or not. The pathway that is subsequently followed by a peat patch or portion thereof is

determined by a number of factors including peatland type. There are 14 pathways, or decision tree branches, in the blanket peatland disintegration pathway model.

A preliminary schematic peatland disintegration pathway model was developed for the common peatland types in the Stephens Lake area. These pathway models include driving factors, pathways between states and rate estimates. Peatland disintegration pathway models for some peatland types were subsequently combined with another pathway model either because statistical analyses indicated they had similar dynamics or because insufficient information was available to develop a separate pathway model. The three broad peatland types used for the peatland breakdown model components are:

- Peat plateau bog (most resistant type).
- Floating peatland including collapse scar (least resistant type and already floating).
- All other peatland types.

The overall peatland disintegration model has four main components:

- Peat resurfacing.
- Reservoir expansion (*i.e.*, peatland and peat mat breakdown).
- Floating peat mat potential mobility.
- Organic sediment released into the aquatic system.

The peatland disintegration is deterministic except for the peat-resurfacing component, which has a stochastic element.

6A.1.2 Proxy Areas Used for Model Development

Proxy areas that provide good examples of how shorelines and flooded peatlands in the Keeyask reservoir area are expected to respond to Project flooding and the subsequent water regime were selected. The key proxy area selection criteria were that they have a similar ecological context, contained large areas of peatlands when they were flooded over 25 years ago and have adequate historical data.

The three proxy areas used to develop and calibrate the peatland disintegration model were Stephens Lake (*i.e.*, the Kettle GS reservoir), the Notigi reservoir and Wuskwatim Lake. Notigi reservoir and Wuskwatim Lake were flooded and water levels subsequently regulated as part of the Churchill River Diversion. Peatland disintegration model development and parameterization relied most heavily on results from Stephens Lake because it is immediately downstream of the proposed Keeyask reservoir, is the most ecologically comparable proxy area and had the best time series of large-scale historical aerial photography.

The historical datasets that were developed to characterize peatland disintegration dynamics consisted of historical peatland time series mapping and soil profile chronosequence transects.

6A.1.2.1 Historical Peatland Disintegration Time Series Mapping

Historical changes in surface peatland area by peatland type were mapped for each proxy area using a time series of large-scale historical stereo air photos. Pre and post-flood ecosite maps for Stephens Lake and the Notigi reservoir areas were photo-interpreted from black and white stereo photos. Historical photo years available for Stephens Lake area included 1962, 1971, 1975, 1982, 1986, 1999, 2003 and 2006. These years represented post-flooding ages -9, 0.2, 4, 15, 28, 32 and 35 years. Historical photo years available for the Notigi reservoir area included 1969, 1978 and 1998. These years represented post-flooding ages -7, 0.8 and 22 years.

Ecosite polygon attributes that were either photo-interpreted or assigned by the GIS were ecosite type, material type (P=peat; M=mineral), island (Y=peat completely surrounded by water; N=peat not completely surrounded by water), and mineral base present (*i.e.,* the mineral material underlying the peat is near or above the water surface level in the photos). These attributes were determined for each polygon at each age because they may change as a peat polygon changes in size and shape over time.

Historical peatland disintegration dynamics for Wuskwatim Lake were reported in the Wuskwatim GS project environmental impact statement.

Within each proxy area, historical peatland disintegration datasets were developed for case study areas. Case study areas were selected to represent different levels of factors thought to be potentially important in determining the nature and rate of peatland disintegration in a particular reservoir. Those driving factors were water temperature, water depth, water current and wave energy. The case study areas captured most of the areas that had large peatlands shortly after initial flooding.

Stephens Lake contained six case studies areas (Map 6A-1). The Notigi reservoir was sub-divided into two general areas on either side of the main Burntwood River channel. The western area was further sub-divided into seven peatland disintegration driving factor zones yielding eight case study areas for the Notigi reservoir (Map 6A-2).

It quickly became apparent during historical air photo interpretation that peat plateau bogs were the keystone peatland type in peatland disintegration dynamics. Peat plateau bogs disintegrate at lower rates than other peatland types and, because they have massive ice cores, they protect other peatland types and mineral shores from breakdown or erosion. Therefore, more a more detailed analysis of peat plateau bogs was undertaken to quantify peat plateau bog bank recession rates and to identify potential influential variables for these dynamics. This examination was based on more precise mapping of peat plateau bogs and measuring bank recession distances between air photo years.

An estimated 56% of unflooded peatlands inside the non-disintegrating limit disintegrated during the first 28 years after flooding at Stephens Lake. The comparable values for Notigi reservoir and Wuskwatim Lake were 51% and 84% for the first 22 years and 24 years after flooding, respectively. Peatland disintegration was expected to continue for many years in all of the proxy areas but at much lower rates than observed in the early years after flooding.

The rate of peat area loss, which is the inverse of reservoir expansion not including mineral erosion, varied greatly across the case study areas. Increasing degrees of connection with and exposure to the

main body of the reservoir was associated with higher rates of peatland disintegration. The case study area in Stephens Lake with the lowest degree of reservoir connection experienced an initial increase in total peat area, which persisted over the 32 year study period (ostensibly due to shallowly flooded peat that resurfaced and expanded in surface area).

The rate of peat area loss also varied greatly with peatland type. Floating peatlands in the initial reservoir generally broke down relatively quickly if they were exposed to moderate or high wave energy. In contrast, peatland types with ground ice had lower disintegration rates. Peat plateau bogs had the lowest disintegration rates since one of their defining characteristics is thick continuous ground ice. It became apparent that peat plateau bogs were the pivotal type in peatland disintegration dynamics. Peat plateau bogs are analogous to a dyke because they create a physical barrier to water percolation, wave energy and current and because they are a thermal barrier to warm lake water. Slowly over time, the ground ice in reservoir peat plateau bogs melts and thereby shrinks the peat plateau bogs to expose other less resistant peatland types. Some of the newly exposed peatlands break down relatively quickly when exposed to wave action. It is thought that mechanism accounting for the relatively low peat plateau bog disintegration rate relates to the surface peat mat and possibly water thermal gradient. This is the same mechanism that prevents collapse scars from expanding and removing peat plateau bogs under natural conditions. The surface peat mat collapses and covers the ground ice thereby insulating the ground ice from warm air and reservoir water. Cold temperatures behind the peat blanket may cool reservoir water adjacent to the peat plateau bog.

6A.1.2.2 Soil Profile Chronosequence Transects

Soil profile data were collected along chronosequence transects in Stephens Lake, the proxy area that is most ecologically comparable to Keeyask. A chronosequence transect is a transect that passes through locations representing different times since peatland disintegration started. The resulting spatial sequence is an analogue for how peatlands change over time after flooding. Chronosequence transects originated in unaffected locations of currently intact peatlands and proceeded out into the open reservoir water passing through several disintegration stages. Open water "soil profiles" provide data relevant for resurfacing, peat bank collapse, peat sinking and sedimentation. Stephens Lake chronosequence transect results were used to confirm proxy area historical mapping results and to develop a better understanding of the mechanisms involved in peatland disintegration.

Soil profiles at over 1,700 locations were sampled along the chronosequence transects. Results from these data confirmed the peatland disintegration patterns derived from the historical time series mapping. These data also showed that massive ice in surface peat plateau bogs was generally not affected beyond 0.5 m from the peat plateau bog bank edge. These data were the primary field data used to estimate peat resurfacing rates by ecosite type.

6A.1.2.3 Model Development

A peatland that escapes initial flooding can pass through several states before sinking to the lake bottom. One example pathway is: intact peatland > collapsed peat mat > floating peat mat > sunken peat mat. In

contrast, some floating peat mats in sheltered locations may expand horizontally and/or vertically as new peat is formed by plants growing on the surface.

The schematic representation of the post-flooding peatland disintegration pathways by ecosite type was revealed by hidden Markov chain analysis of Stephens Lake historical peat area time series data (see Figure 6A-1 for an example). A total of 117 different peatland disintegration pathways were observed for the five post-flooding ages and seven pre-flood peat ecosite types. Transition percentages from the hidden Markov chain analysis identified the most common peatland disintegration pathways for each pre-flood peatland type. That is, the ones that would be considered during model development. These pathways were confirmed by available information from other proxy areas and studies of Hydro Quebec reservoirs

Statistical analyses of proxy area historical mapping data were conducted to help determine which variables influenced the pathway followed by a particular peat patch and the relative degrees of influence of these driving factors. These statistical analyses found that peatland disintegration dynamics were significantly affected by wave energy, location, island, distance from water, reservoir exposure and patch area. These variables appear to collectively represent reservoir exposure at the bay and patch spatial levels. Increasing reservoir exposure increased the likelihood that a peat patch transitioned to a more degraded type as well as the mean rate associated with those transitions. Important variables for peat plateau bog disintegration dynamics in addition to those identified for all peatland types included mineral base near water surface and patch morphology. Peat plateau bogs with a mineral base near the water surface had much lower disintegration rates, all other things being equal. Peat plateau bog peninsulas had the highest mean disintegration rates.

6A.1.3 Peat Resurfacing

The amounts and types of peat that resurface during each prediction period are determined by: (a) a peat mat's resurfacing likelihood; (b) random selection; and, (c) the estimated proportion of the peatland area that resurfaces after flooding. Rates of reservoir filling and month of flooding were not included as factors in the peat resurfacing component of the peatland disintegration model. Flooding is planned for the fall and is expected to occur relatively quickly with no subsequent large draw downs outside of the normal operating range.

A peat mat's resurfacing likelihood was determined by its resurfacing potential as counteracted by hydrostatic pressure. Peat mat resurfacing potential was determined for each peatland type by typical buoyancy and degree of anchoring. Lab work was conducted to better understand flooded peat buoyancy and resurfacing potential. Physical properties of peat and peat buoyancy parameters were measured and characterized using peat samples collected in the Keeyask reservoir area. Lab work found that fibric layer (*i.e.*, Of layer) saturated apparent specific gravity did not vary with peatland type. Therefore, buoyancy for each peatland type was derived from a combination of mean of thickness and percentage of peatland area with a surface of layer. Degree of anchoring for each peatland type was a professional judgment based on the study results, field experience and the limited available literature. Aquatic and collapse scar peatlands had the highest resurfacing potentials while veneer bogs and blanket peatlands had the lowest. Peat plateau bogs were intermediate.

Hydrostatic pressure was incorporated as a linear function of water depth. The counteracting effect was nil at a water depth of 0 m and complete at a water depth of 6 m. Peatlands in water deeper than 6 m are permanently flooded in the model.

Peat mat resurfacing likelihood was determined by this equation:

- Peat Mat Resurfacing Likelihood = Resurfacing potential for peatland type * Hydrostatic pressure effect

or

- Peat Mat Resurfacing Likelihood = Resurfacing potential for peatland type * (1- Water Depth * 0.1667)

The peat resurfacing component of the peatland disintegration model includes a probabilistic element. There was no strong basis for determining which particular peat mats will resurface during a modelling period due to the lack of appropriate monitoring data from any flooded area in northern Canada. Therefore, polygons that resurface during a prediction period are randomly selected provided their peat mat resurfacing likelihood exceeds a minimum value. This minimum value was based on the estimated proportion of peatland area that resurfaces after flooding.

The proportion of peatland area that resurfaces after flooding was derived from the Stephens Lake historical mapping, lab results, field experience and relevant literature. The data based estimate of the percentage of peatland area that resurfaced in the Stephens Lake was between 42% and 75%. This range could not be used as a benchmark for Keeyask because there are important differences between the Keeyask and Stephens Lake initial conditions and driving factors that are expected to result in substantially lower resurfacing in the Keeyask reservoir. A benchmark range of 35% to 45% for total resurfacing area was used for model calibration. This benchmark was used loosely because the Keeyask and Stephens Lake differ with regard to water depth, operating range and ecosite composition (each peatland type has a different resurfacing potential). Pre-flood ecosite composition, peat mat resurfacing likelihood by peatland type and water depth are the most important influences on the types and amounts of resurfacing.

The available information suggests that resurfacing ceases within 5 to 10 years of flooding. Anaerobic microbial decomposition in submerged peat generates gas bubbles, which can increase buoyancy over time if the bubbles become trapped in the peat matrix. However, microbial decomposition rates should decline over time as labile material is consumed. In addition, sedimentation adds surface weight to the submerged peat mat and, along with the sustained effects of hydrostatic pressure, counteracts initial and ongoing buoyancy.

6A.1.4 Surface Peatland and Floating Peat Mat Disintegration

Distance from reservoir surface water edge, whether or not it was an island and wave energy determined how quickly and which peatlands/peat mats changed during a prediction period. The rates associated with these variables differed by broad peatland type.

6A.1.5 Floating Peat Mat Potential Mobility

Field and lab results indicated that where peat mats resurface it is only the Of layer of the flooded peat that resurfaces. The median thickness of recently resurfaced peat mats is 0.9 m. Peat mats that resurface in water deeper than 1 m are classified as mobile.

6A.1.6 Organic Sediment

Areas of disintegrated peat generated by the surface peatland breakdown/formation and resurfacing components of the peatland disintegration model were converted into organic sediment volumes and masses. Volumes were estimated for each organic layer as surface area multiplied by median layer thickness for the peatland type as estimated from study area field data. The latter values were derived from over 800 soil profiles sampled in the Keeyask reservoir area. The model converts peat volumes to masses based on bulk density values measured in the lab from peat samples collected in the Keeyask reservoir area. Mass estimates are broken down into mats, chunks, fibres and particles as well as whether the material is floating, suspended in the water column or sunken. The distribution of material between these classes is based on lab measured values.

6A.1.7 Model Assumptions

The peatland disintegration model does not incorporate either future climate change effects or indirect peatland changes that result from the "domino effect" external to the reservoir bounding condition. Domino effect predictions are provided in the terrestrial habitat and ecosystems assessment since virtually none of this peat material is expected to enter the aquatic system.

6A.1.8 Model Validation

Two approaches were taken model to validation given the lack of relevant monitoring data from other flooded areas and the lack of previous attempts to predict shoreline and floating peat breakdown. In the first approach, the peatland disintegration model was run on pre-flood Stephens Lake conditions to determine the extent to which the model could replicate actual peatland disintegration for this area. The Stephens Lake area pre-flood ecosite map defined initial conditions. From this starting dataset, the peatland disintegration model was run for 32 years. Model predicted conditions compared favourably with actual Stephens Lake conditions.

Peat plateau bogs were the peatland type of most concern in the validation because this is the pivotal ecosite type overall peatland disintegration dynamics. Very good post-hoc monitoring peat plateau bog data was available for Stephens Lake from historical air photo interpretation.

Model performance for peat plateau bogs was very good (Table 6A.1-1). The mean difference between actual and predicted area over the four prediction periods is 6.8%. More importantly, the locations where the model predicts that peat plateau bog disintegration will be either rapid or slow are the same as what actually occurred in the Stephens Lake. Age 15 had the largest deviation between predicted and actual area at 14% but this was also the worst year for aerial photos (*i.e.*, the monitoring data was thought to

overestimate the amount of peat in all classes for this age). Also, the model predicted the disappearance of one larger peat plateau bog that has actually survived 32 years. According to field data, the discrepancy occurs because the peatland disintegration model does not include mineral base as a variable and this peat plateau bog has a prominent mineral base.

Validation results were poor for floating peatlands. This was expected given that we have no suitable monitoring data from Stephens Lake. Peat mats that float to the surface can sink or move large distances within days or weeks. Air photos taken years apart cannot monitor this type of dynamic. Very short interval monitoring data commencing shortly after flooding would be needed to quantify floating mat mobility.

Table 6A.1-1: Stephens Lake Validation: Predicted and Actual Areas and Deviations Between Predicted and Actual Values for Peat Plateau Bogs

Age	Area (ha)			Percent Difference	
	Actual	Predicted	Difference	Actual	Absolute
4	259	250	9	3.5	3.5
15	240	207	33	13.8	13.8
28	180	185	-5	-2.8	2.8
32	169	181	-12	-7.1	7.1
Mean Absolute			6.3		6.8

Results were good for the remaining peatland types (Table 6A.1-2). The model generally predicts more area remaining than actual but this seemed reasonable because Stephens Lake had a higher range of water elevation fluctuation than planned for Keeyask and because trees were not cleared prior to flooding.

The overall spatio temporal patterns of peatland disintegration by ecosite type corresponded fairly well.

Table 6A.1-2: Stephens Lake Model Validation: Predicted and Actual Areas and Deviations Between Predicted and Actual Values for Ecosites and Other than Peat Plateau Bogs

		Age			
Ecosite		4	15	28	32
Veneer Bog	Actual ha	60	57	9	3
	Predicted ha	50	25	17	15
	Difference ha	9	33	-8	-12
	% Difference	16	57	-87	-379*
Blanket Peatland	Actual ha	220	197	68	61
	Predicted ha	271	208	155	143
	Difference ha	-51	-11	-87	-82
	% Difference	-23	-6	-128	-134

The second approach to model validation was sensitivity analysis. Model parameter coefficients were varied from the 50th percentile values obtained from the study results. For the sensitivity analysis, model states and parameter coefficients were set to their 95th percentile values.

6A.2 MINERAL EROSION

6A.2.1 Future Erosion Without the Project

Future bank recession rates without the Project are based on historical recession rates in the study area measured from historical air photos dated 1986 to 2006 and from shore zone transects surveyed in the summers of 2006 and 2007.

Historical top-of-bank positions were mapped along the entire shore zone length within the study area from 1986, 1999, 2003 and 2006 aerial photographs. The 2003 and 2006 aerial images are orthorectified, while the 1986 and 1999 air photos are georeferenced. Top of bank positions for each year were overlaid in the GIS and compared in order to select data sets that would form the basis for projection of future recession rates without the Project.

Estimates of future mineral erosion without the Project include the volume and mass of mineral soil that will be eroded from nearshore slopes below the toe of bank.

Figure 6.1-2 (Section 6.1) illustrates a typical eroding shore zone profile.

Historical average annual bank recession rates were determined by measuring the horizontal distance between successive top-of-bank positions on the historical air photos and dividing that distance by the number of years over which the change in bank position occurred. Top-of-bank positions were mapped by heads-up digitizing combined with reference to stereoscopic contact aerial photographs to determine

the top-of-bank position. Historical average annual bank recession rates were measured around the entire study area shoreline and mapped in 0.25 m/y increments. The resulting map shows historical average annual recession rates along the shoreline as being within a minimum and maximum range based on the historical bank positions mapped from the aerial photographs.

Future bank positions were projected by multiplying the historical average annual recession rate by particular time intervals into the future. To arrive at a most likely projection of future bank positions, average annual recession rates were used for this calculation (*i.e.*, an average rate of 0.375 m/y was used for shoreline segments where the recession rate was within the range 0.25 m/y to 0.5 m/y). To compare without project bank recession projections to with project projections, it is necessary to first predict the amount of recession that would likely occur from the time of the 2006 aerial photographs to the proposed project in-service date of 2019. Further projections are then made for 1 year (*i.e.*, 2019 to 2020), 1 to 5 years (2020 to 2024), 5 to 15 years (2024 to 2034), and 15 to 30 years (2034 to 2049) after the proposed in-service date. These time intervals correspond to intervals that have been used for predicting future bank recession with the Project. Projected future bank positions are plotted in GIS shape files for comparison with other spatial data sets.

The volume of mineral soil eroded due to shore erosion for each time interval was estimated by multiplying the predicted bank recession distance by the bank height, and then adding the estimated volume of nearshore mineral erosion. Bank height is taken from a field mapping data set produced by ECOSTEM (GN-9.2.1), with shoreline video coverage used where needed to fill data gaps. No attempt was made to predict changes in bank height with time because the positional accuracy of data sources that could be used to make such predictions (*i.e.*, digital elevation models and air photo coverage) is likely less than the accuracy of assuming that changes in bank height will be relatively small. The texture of eroded mineral soil is classified as either coarse-textured or fine-textured mineral soil based on shoreline bank material mapping by ECOSTEM in 2003. Coarse textured soil includes till and glaciofluvial sediments. Fine textured soils are dominantly glaciolacustrine clays and silts. Typical grain size distribution curves for fine and coarse textured materials are shown in Figure 6A.2-2. Peat and bedrock were also mapped by ECOSTEM (GN-9.2.1). Bedrock-controlled shorelines are assumed to be non-erodible. Composition of all eroding banks are assumed to remain the same throughout the modelling period.

In areas with peat banks, criteria were developed in collaboration with ECOSTEM to determine how future recession of peat banks would be addressed. That is, which shore segments in the existing environment would undergo mineral erosion rather than peatland disintegration processes. Places where the interface between peat bank and the underlying mineral or bedrock material was near or above the water level were addressed by mineral erosion processes. All other peat bank shore segments were addressed by peatland disintegration processes.

To estimate erosion from the nearshore, it is necessary to first identify those nearshore areas that are likely to erode and those that are likely to be stable. The erodibility of the nearshore material depends on the material texture and the flow velocity or wave action to which the material will be exposed. Texture of nearshore materials was determined from the beach material classification. Materials such as bedrock, cobbles and peat are assumed to be non-eroding. Fine-grained materials such as sand and clay will be

subject to erosion, depending on flow velocity and wave energy conditions. It was also assumed that no nearshore erosion will occur along shoreline segments where the bank was found to be stable based on historical air photo analysis.

A second step required to determine the erodibility of nearshore mineral soil is to assess the flow velocity and wave action to which a particular shoreline segment may be exposed. Future flow velocities without the Project were based on 50th percentile flow conditions. The relationship from Hjulstrom (1935) (see Figure 6A.2-3) was used to determine threshold nearshore flow velocities for clay (1 m/s) and sand (0.1 m/s) to begin to move due to current flow. Where nearshore velocities are below these thresholds, it is assumed that erosion will be driven by waves.

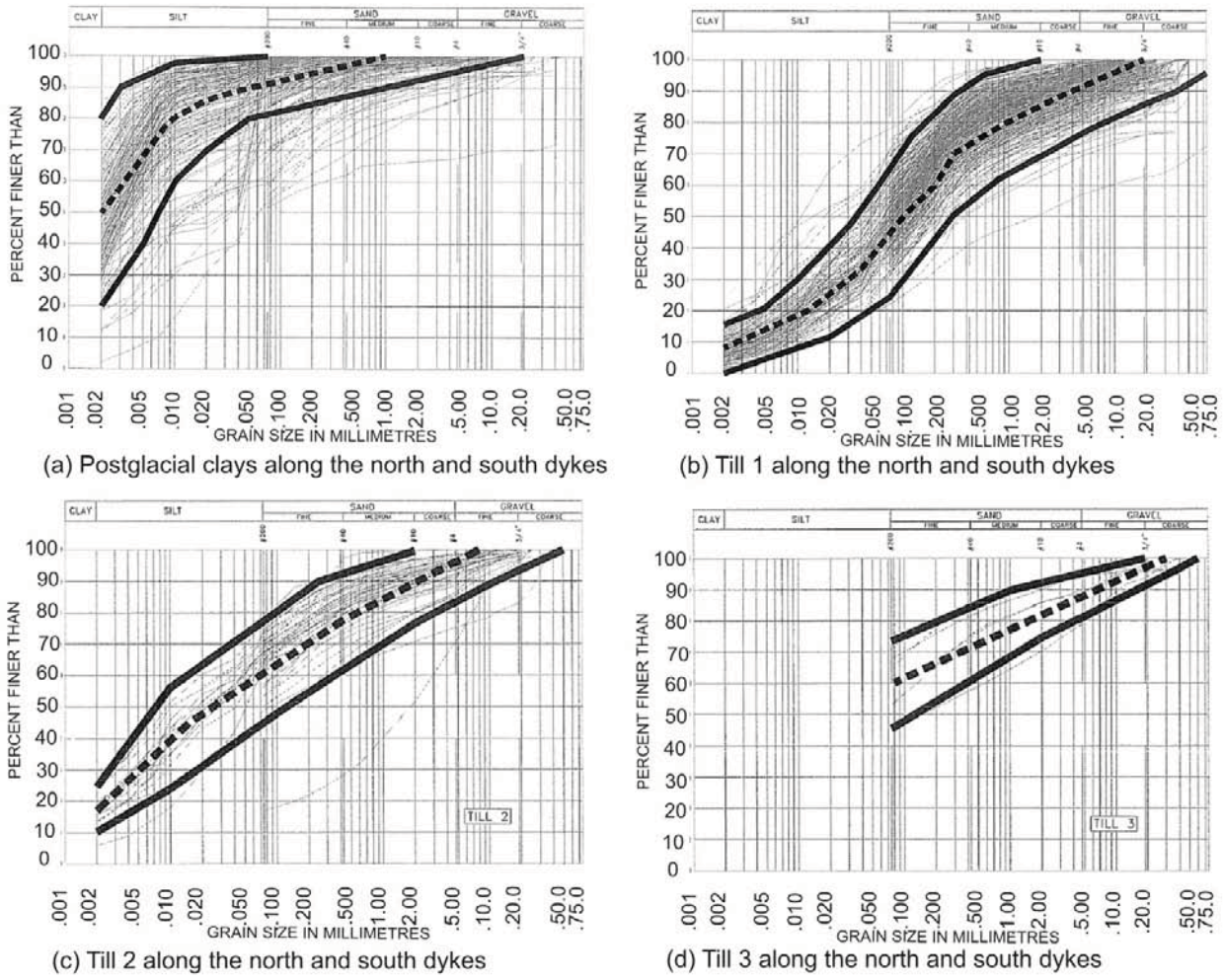

Figure 6A.2-2: Typical Grain Size Distribution Curves for Coarse and Fine Textured Mineral Soils in the Keeyask Area

In areas subject to nearshore erosion due to flow, the volume of nearshore erosion is estimated by assuming that erosion will occur from the 50th percentile shoreline to a depth of 3 m, constrained laterally

by the bank recession distance predicted from historical erosion rates, as illustrated (in Figure 6A.2-5). The 3 m depth is consistent with the definition of nearshore for aquatic studies.

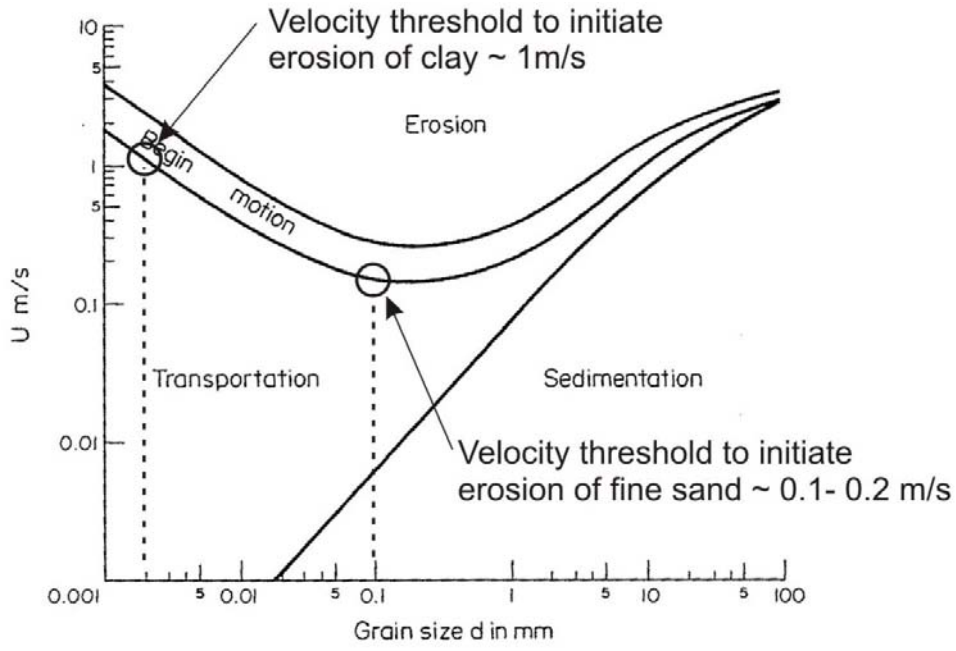

Figure 6A.2-3: Hjulstrom (1935) Diagram Illustrating Flow Velocity Thresholds for Clay and Fine Sand

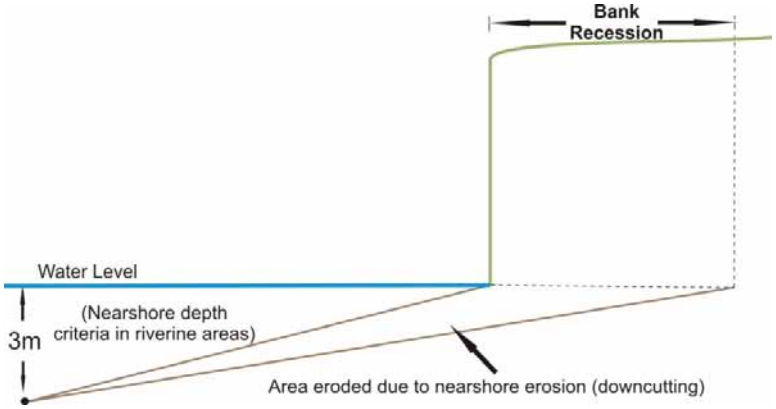

Figure 6A.2-4: Method Used to Determine Nearshore Erosion Along Riverine Shorelines – Existing Environment

In areas subject to nearshore erosion due to waves, the volume of nearshore erosion is estimated by assuming that erosion will occur from the 50th percentile shoreline to a depth of 2 m (approximate maximum wave base depth), constrained laterally by the bank recession distance predicted from historical erosion rates, as illustrated (in Figure 6A.2-5).

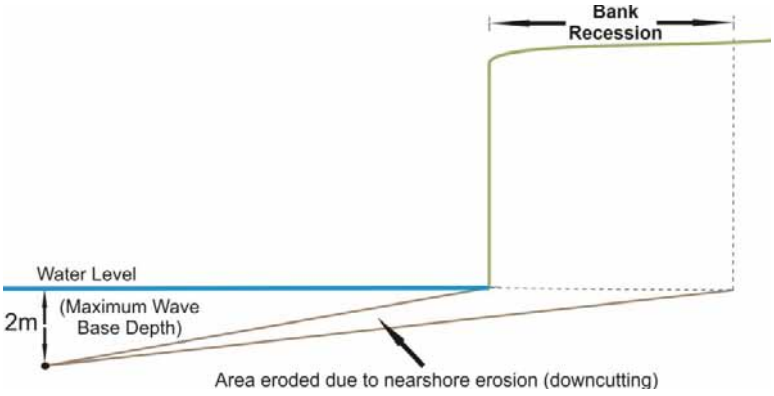

Figure 6A.2-5: Method Used to Determine Nearshore Erosion Along Wave Dominated Shorelines – Existing Environment

Estimated volumes of eroded fine-textured mineral soil, coarse-textured mineral soil and peat for each time interval are reported by shore zone reach to assist assessment of environmental impacts.

6A.2.2 Future Erosion With the Project

Future mineral erosion rates with the Project are based on application of a GIS-based computer model designed to predict the volume and mass of mineral soil that will be eroded from the shore zone under peaking and base loaded modes of operation, as well as future bank recession distances. Application of this model takes advantage of knowledge gained from past studies in northern Manitoba and elsewhere where it is currently being applied on similar projects. In addition, local site specific data have been collected to ensure that the model accurately reflects processes and conditions in the Keeyask study area. Important sources for such information are data collection sites in Stephens Lake. Stephens Lake was impounded in 1971 following construction of the Kettle GS. The terrain setting and shoreline materials in Stephens Lake are similar to conditions that will develop in the proposed Keeyask reservoir. Therefore, shoreline erosion processes and rates in Stephens Lake serve as a valuable proxy for the Keeyask reservoir.

The following specific physical environment data sets are required to implement the GIS mineral erosion model:

- Mean nearshore and above shore (bank) slopes determined from the digital terrain model.
- Wave energy determined from 2-D wave modelling (requires fetch measured from the reservoir polygon and wave data from the Environment Canada station at Gillam).
- Shore zone material derived from shore zone classification, terrain mapping and field exploration.
- Erodibility coefficients for shore zone materials determined from calibration sites in Stephens Lake.
- Water level fluctuation range derived by Manitoba Hydro from hydraulic models for peaking and base loaded modes of operation.

- Average or typical ice freeze-up and ice break-up dates to define the ice-free period during which waves can occur.
- Nature of ice cover (thermal cover in the main part of the reservoir; mechanical cover and border ice in narrow riverine reaches).

6A.2.3 The Erosion Process

Key components of the shore erosion process simulated in the numerical model are wave action, water level fluctuation due to peaking (~1 m weekly fluctuation) and base loaded (stable water level) modes of operation, nearshore down cutting and bank recession.

Nearshore down cutting occurs on submerged nearshore slopes where water depths are less than the maximum wave base depth. Bank recession results from bank mass wasting caused by over steepening of bank slopes due to toe of bank erosion. Toe of bank erosion, in turn, can result from gradual nearshore down cutting of the nearshore slope, or by direct wave erosion of the bank toe when water levels are high. Fluctuating water levels under a peaking mode of operation have the effect of widening the nearshore slope over which down cutting occurs, but still periodically exposing the toe of bank to direct wave action when water levels are high.

For a base loaded mode of operation, waves are able to reach the bank toe 100% of the time (during the open water season). Therefore both toe of bank erosion and nearshore down cutting occur at all times (except when winds are calm) under base loaded conditions.

For a peaking mode of operation, water levels fluctuate over a 1 m vertical operating range. Therefore, toe of bank erosion and nearshore down cutting can only occur when water levels are near the upper end of the range. When water levels are lower than FSL, waves are unable to reach the bank toe and erosion occurs by nearshore down cutting.

In addition to differences in whether erosion is dominated by toe of bank erosion or nearshore down cutting for peaking and base loaded modes of operation, bank materials usually have different erodibility characteristics than beach materials. This is the case because erosion of the bank includes erosion of intact material at the bank toe, as well as erosion of colluvium that accumulates at the bank toe due to bank weathering and mass wasting mechanisms. While the erodibility of the intact bank material may be similar to the erodibility of similar materials located on the beach (although in some cases beach and bluff materials may be quite different), the erodibility of colluvium derived from the bank is generally much higher than that of in situ bank and beach material. As a result, erosion of the bank (consisting of in situ bank material and colluvium) tends to result in larger volumetric erosion rates than erosion of the nearshore slope for similar wave energy environments.

In addition to these differences, the way in which the wave energy is dissipated on the nearshore slope differs from how wave energy is dissipated at the bank toe. Energy dissipation on the nearshore slope is relatively gentle in nature, with fairly uniform dissipation of energy over a relatively broad area. By comparison, energy dissipation at the bank toe is more turbulent and concentrated over a relatively small area. More turbulent, concentrated energy dissipation at the bank toe usually results in a greater loss of material for a given total amount of energy dissipated.

Potential for ice processes to affect shoreline erosion is largely restricted to parts of the reservoir where a mechanical ice cover may form in narrow riverine reaches where the impact of ice processes in the future with the Project will be similar to their effect under existing conditions. The effect of mechanical ice processes on erosion in these areas is not directly taken into account by the erosion model. Therefore, model results are considered together with historical erosion rates and shore zone material types to arrive at predictions of future erosion rates with the Project in these areas.

6A.2.4 Modelling the Erosion Process

The erosion model is based on the observation that the volume of sediment eroded from a shore zone by wave action is directly proportional to the effective wave energy density reaching the shore zone. When plotted on a graph, the linear gradient of this relationship is defined as the erodibility coefficient, and is a characteristic property of the shore material type. This relationship was verified at 19 calibration sites in Stephens Lake. It has also been demonstrated by Newbury and McCullough (1984) at Southern Indian Lake and by Penner (1993 and 2007) at four reservoirs in southern Saskatchewan. The basis for this relationship was published by Kachugin (1966). Although factors other than wave action may contribute to bank recession at specific locations, wind generated waves are the dominant force causing bank recession in lakes and reservoirs (Reid 1988).

Prediction of future volumetric erosion and bank recession rates with the Project are based on the relationship between effective wave energy density and volumetric erosion rate, discussed above, following the approach described by Penner (1993). However, Penner's approach has been modified in some aspects to better predict wave energy dissipation on nearshore slopes and to allow different water level fluctuation ranges to be incorporated in the model. Accordingly, development of the Keeyask mineral erosion model entails the following:

- Determining the effective wave energy density at a particular site or shoreline reach.
- Calculating volumetric erosion as the product of effective wave energy and erodibility coefficient.
- Determining the bank recession distance in accordance with the volume of mineral soil predicted to erode.

Further information on erosion processes in lakes and reservoirs can be found in the following references: Reid (1984); Newbury and McCullough (1984); Davidson-Arnott (1986); Kamphuis (1986); Mollard (1986); Reid *et al.,* (1988); Kamphius (1990); Bishop *et al.,* (1992); Nairn (1992); Penner *et al.,* (1992); Penner (1993a, b, c); Davidson-Arnott *et al.,* (1999); Davidson-Arnott and Ollerhead (1995); Amin and Davidson-Arnott (1995); Davidson-Arnott and Langham (2000); Penner and Boals (2000); Penner (2002) and Zimmer *et al.,* (2004).

6A.2.5 Effective Wave Energy Density

Effective wave energy density is the portion of total deepwater wave energy dissipated per unit area of the shore zone. The portion of the shore zone affected by wave action is located between the maximum

wave base depth at the minimum water level and the upper elevation of the wave run-up and wind set up at the maximum water level. This zone is shown schematically (in Figure 6A.2-6).

Effective wave energy density reaching the shore per unit length of shoreline is calculated as the total deepwater wave energy density divided by the area of the shore zone affected by wave action. This area per unit of shoreline length is calculated as the water level fluctuation range plus the average wave base depth (*i.e.*, the wave base depth for average wave conditions) divided by the sine of the nearshore slope angle, plus the width of the wave front dissipation zone (which takes into account wave base depth, wave run-up and wind set up).

Water level range for the Keeyask reservoir has been predicted for the expected range of potential flow conditions for a weekly peaking mode of operation as well as a base loaded mode of operation. To arrive at predictions of the most likely shore erosion volumes and bank recession distances, the water level range of 1 m (reservoir level varying from 158 m to 159 m) has been used for a peaking mode of operation and a fluctuation range of 0 m (stable reservoir level at 159 m) has been used for a base loaded mode of operation. Water level duration curves for the Keeyask reservoir are shown (in Figure 6A-6). All other factors being the same, effective wave energy will be lower for a peaking mode of operation as compared to a base loaded mode of operation because the water level fluctuation range is larger for a peaking mode of operation. This results in the dissipation of wave energy over a wider nearshore zone than would occur in a base loaded mode of operation.

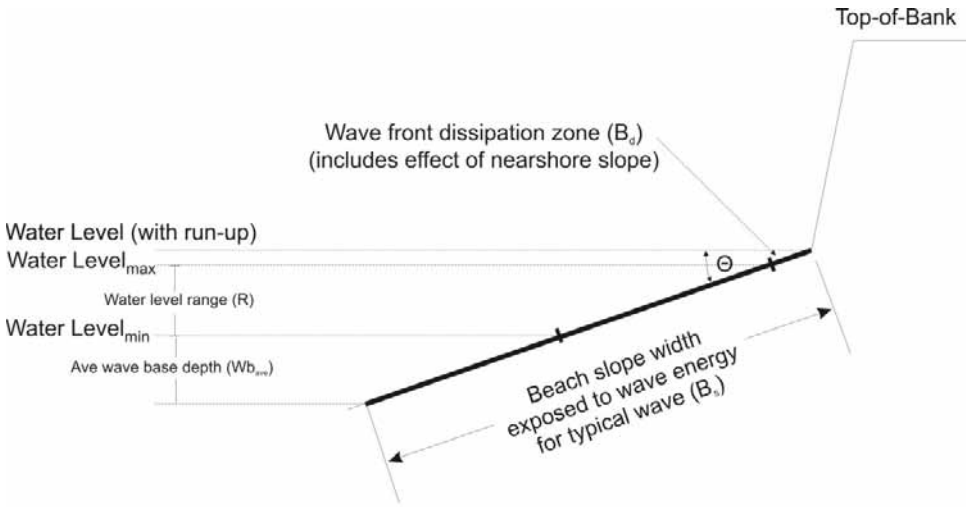

Total deep water wave energy (We_{tot})

Water level range (R) = Water level$_{max}$ - Water level$_{min}$

Average wave base depth for typical wave (Wb_{ave})

Beach slope width exposed to wave energy dissipation (B_s) = B_d + (R + Wb_{ave})/sinθ

Effective wave energy (We_{eff}) = We_{tot}/(B_s) = We_{tot}/ (B_d + (R + Wb_{ave})/sinθ)

Figure 6A.2-6: Schematic Shore Zone Profile Illustrating Parameters Affecting the Calculation of Effective Wave Energy

Deepwater wave energy has been determined for the proposed Keeyask reservoir using the numerical model STWAVE, a two-dimensional wave generation and propagation model that was developed by the US Army Corps of Engineers. The model includes wind wave generation, refraction, shoaling, breaking and has a limited implementation of wave diffraction. The model is run on a regularly spaced 40 m grid. Different grids were prepared for the model, to simulate the wind and waves from 22.5 sectors around the compass (*e.g.,* N, NNE, NE, etc.) for a total of 16 grids. For each grid, waves were predicted at wind speeds of 5, 10, 15, 20 and 25 m/s, resulting in a total of 80 simulations.

STWAVE is a steady state wave model and relies on the assumption that the winds are blowing for a sufficient temporal duration to create a steady state wave field. This is generally true for the Keeyask study area since the longest open fetches are typically in the range of 15 km. Because STWAVE is not a transient model, the initial boundary conditions are not relevant.

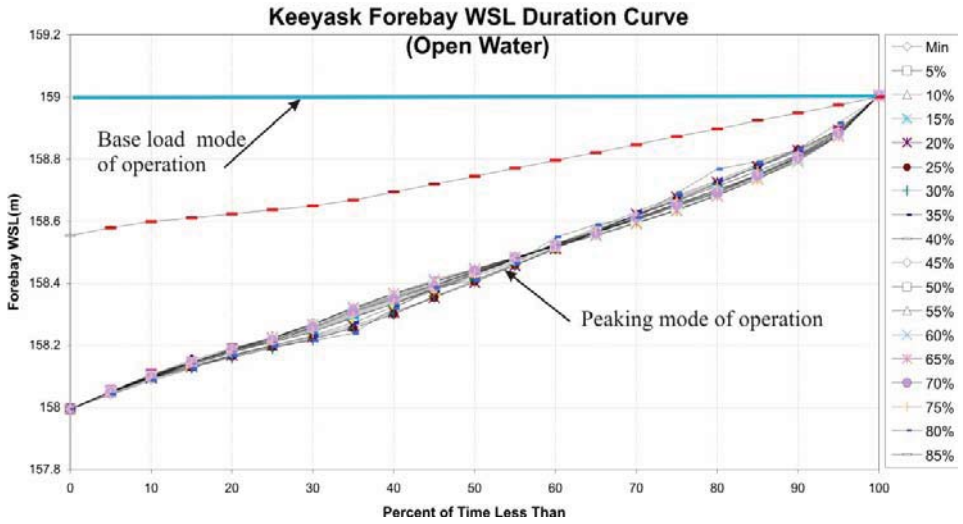

Figure 6A.2-7: Open Water Keeyask Reservoir Water Surface Level (WSL) Duration Curves

Hourly wind data from the Gillam station for the period 1971 to 2004 were used in the model. A wind scaling factor was applied to adjust for higher wind speeds over water than over land. Hourly wave conditions are determined from the hourly wind data for the plan view and bathymetric geometry of the reservoir using an ArcGIS application. The hourly wave file includes direction, wave height and wave period for each grid location for each hour.

After the hourly wave file was generated, wave energy density at selected grid locations was determined using the ESWave computer application. ESWave, developed by Baird and Associates, reads the hourly wave file and calculates wave energy density as well as providing visualization tools to evaluate the data, including wave roses, tabular summaries and storm listings. For the Keeyask Project, annual deepwater wave energy density was calculated using the standard equation that accounts for the density of water, gravitational acceleration and the wave height.

6A.2.6 Erodibility Coefficients

Erodible mineral soil materials in the Keeyask reservoir shore zone consist primarily of coarse-textured till and glaciofluvial sediments and fine-textured glaciolacustrine sediments. Typical grain-size distribution curves for these types of sediments are presented in Figure 6.A.2-2. Because the Keeyask study area is located in the widespread discontinuous permafrost region, mineral oils in the shore zone will be affected by permafrost in some locations. However, permafrost will most commonly occur in certain types of peatlands, with occurrences in mineral soil being sporadic and localized in extent. The types of materials and permafrost conditions found in the Keeyask study area are similar in nature to permafrost occurrences around the Stephens Lake shore zone. Moreover, shore zone slopes and bank heights similar to what are expected in the proposed Keeyask reservoir also occur in Stephens Lake.

Because of these similarities, combined with the fact that Stephens Lake is an impounded waterbody, the Stephens Lake shore zone serves as a useful proxy for the Keeyask Project and thus provides valuable information to determine appropriate erodibility coefficients for use in the Keeyask erosion model application. Therefore, 19 model calibration sites were identified in Stephens Lake to provide information on the erodibility of fine and coarse textured mineral soil. These sites also reflect the potential influence of permafrost conditions on the erodibility of mineral soil banks to the extent that permafrost is present at these sites. Erodibility coefficients for coarse and fine textured mineral soils are defined by the slopes of the lines (in Figure 6A.2-8).

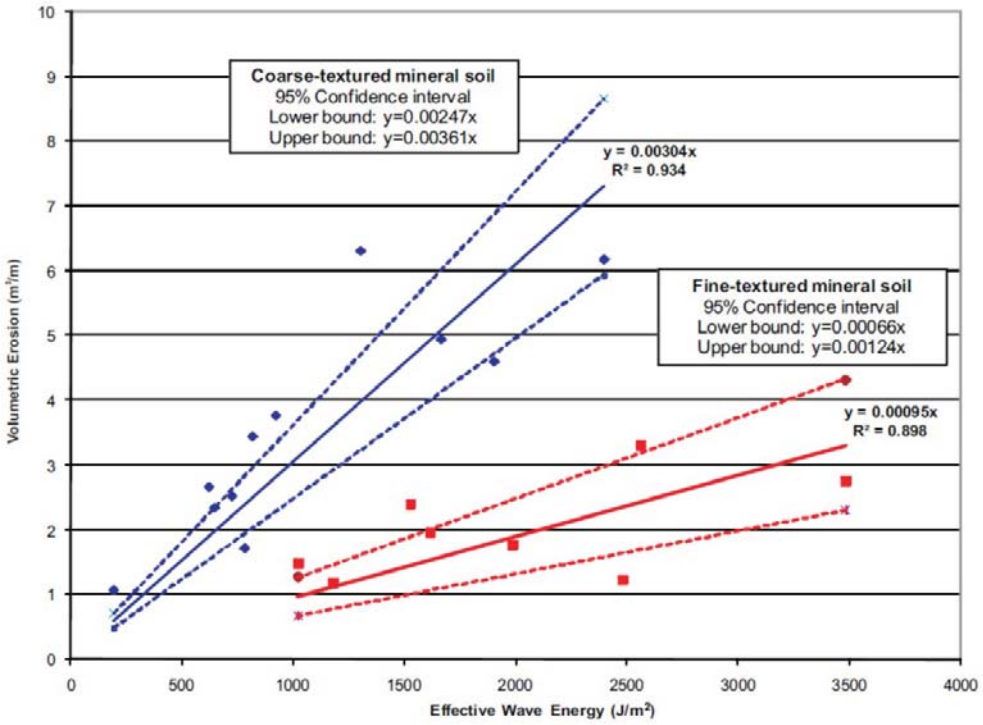

Figure 6A.2-8: Erodibility Coefficients for Coarse Textured (Blue Line) and Fine Textured (Red Line) Mineral Soils at Stephens Lake Calibration Sites

The steeper the slope, the higher the volume of sediment that can be eroded by a given effective wave energy and the greater the erodibility coefficient. Erodibility of a material is related to both the size of the material, how easily the material loosens and breaks apart when exposed to wave energy and by the amount of abrasion that occurs on the nearshore slope. Fine grained sediments are more easily transported by wave action but have a higher cohesion and lower sand content, which reduces abrasion. Coarse textured materials have a higher percentage of coarse particles (*i.e.*, sand, gravel and cobbles), which require more energy to be transported but they have lower cohesion and are more susceptible to abrasion. Coarse textured sediments also contain a significant percentage of silt and clay, which can be easily transported by wave action. The erodibility coefficient analysis shown in Figure 6A.2-8 indicates that the lower cohesion and increased abrasion in coarse-textured sediments results in these sediments being more susceptible to erosion (*i.e.*, higher erodibility coefficient) than the fine textured sediments.

To apply the erodibility coefficient in the erosion model, the annual volumetric erosion rate is determined by multiplying the annual effective wave energy density at a site by the erodibility coefficient for the bank material at that site. Effective wave energy density is adjusted annually in the erosion model to account for gradual flattening of the nearshore slope by nearshore down cutting.

Erodibility coefficients determined for fine- and coarse-textured materials are listed in Table 6A.2-1.

Table 6A.2-1: Erodibility Coefficients Determine for Shore Materials at Stephens Lake Calibration Sites

Material Type	Average Erodibility Coefficient ($m^3/J/m^2$)	Upper Limited of 95th Percentile Conference Limit ($m^3/J/m^2$)	Lower Limit of 95th Percentile Confidence Limit ($m^3/J/m^2$)
Coarse Textured Mineral Soil	0.00304	0.00361	0.00247
Fine Textured Mineral Soil	0.00095	0.00124	0.00066

6A.2.7 Volumetric Erosion Rate

The annual volumetric erosion rate is the product of the annual effective wave energy density and the erodibility coefficient of the shore zone material.

6A.2.8 Bank Recession Distance

For a given time step, the predicted bank recession distance is determined from the volumetric erosion rate for that time step and the shore zone profile geometry. To model this process, the shore zone geometry is divided into two components: the nearshore component, located below the maximum water level; and the bank component, located above the maximum water level (see Figure 6.1-2). The model is run iteratively by adjusting the nearshore slope in 0.001 degree intervals and calculating the corresponding increase in cross-sectional area (area= volume/unit length of shoreline) "eroded" from the nearshore and bank slopes. The model cycles through iterative calculations until the "eroded" area equals

the volumetric erosion rate calculated for that time step. When this occurs, the model returns the value of the new nearshore slope and the corresponding bank recession distance. The new nearshore slope is then used as the starting point for calculating the effective wave energy and bank recession for the next time step.

To implement the model, predetermined values are assigned for the minimum nearshore slope angle and the bank slope angle. Values for these two parameters have been determined from field surveyed shore zone profiles in Wuskwatim Lake and Stephens Lake. Based on these data, a minimum nearshore slope of 4^{o} and a vertical bank slope have been used in the model.

6A.2.9 Shoreline Segments

Input parameters required for the model are assigned as attributes to the segmented shoreline in the GIS. Necessary attributes for each segment include segment length, total annual wave energy density, initial nearshore slope, above shore (bank) slope and material type. Segment length is calculated internally by the GIS. Nearshore slope is determined as the average slope below the Year 0 shoreline (*i.e.*, the shoreline that will develop under initial flooding of the reservoir) to a water depth of 2 m (approximate maximum wave base depth). Above shore slope is determined as the average slope within a 75 m wide buffer above the Year 0 + 1 day shoreline (*i.e.*, the modified shoreline that will develop quickly after initial flooding due to movement of floating peatlands and rapid peat disintegration).

6A.2.10 Wave-based and Riverine Erosion in the Future with Project

The wave-based GIS erosion model has been applied throughout the hydraulic zone of influence upstream of the Project. However, along shorelines that are located progressively farther upstream, the post-project environment gradually transitions from a lake environment in the Gull Lake area immediately upstream of the Project to a river environment upstream of Birthday Rapids where the Project will have little impact on water levels and flow velocities. Lake and river shorelines are defined here based on whether waves (lake) or current flow (river) will dominate the shore erosion process.

With and without project nearshore flow velocities, as predicted by hydrodynamic modelling, have been compared and assessed to ensure that erosion model results properly capture future erosion due to wave, riverine and ice processes.

6A.3 MODEL VALIDATION

6A.3.1 Introduction

The Keeyask erosion model has been validated using historical bank recession data from Gull Lake. Two historical periods were used for this analysis: 1) erosion transect data from 2006 and 2007 at selected transect sites in Gull Lake; and 2) historical bank recession distances for the period 1986 to 2006 measured from historical air photos.

6A.3.2 Methodology

Bank recession distances for each validation period were measured from shore zone profiles surveyed in the summer field seasons for the 2006 to 2007 period and from historical air photos for the 1986 to 2006 period.

Wave energy for this period was determined using hourly wind data recorded at Environment Canada's Gillam station for each validation period.

Water level fluctuation range was determined from daily water levels reported at Broken Boat and Box Creek gauge.

Nearshore slope angles were measured from the surveyed shore zone profiles (2006 to 2007) and from a digital elevation model (1986 to 2006). It was assumed that the nearshore slope angle did not change over the validation periods.

An erodibility coefficient of 0.00304 $m^3/J/m^2$ was used for coarse-textured materials and 0.00095 $m^3/J/m^2$ for fine-textured bank materials in the initial validation run. These are the erodibility coefficients that were used in the original model predictions.

Two additional model validation runs were carried out in which erodibility coefficients assigned to fine and coarse textured materials were reduced by 25% and 50%. This was done to investigate the possibility that erodibility coefficients used for model predictions (*i.e.*, representing erodibility conditions in a new reservoir) may be higher than erodibility coefficients for beach and bank materials in the existing mature Gull Lake shore zone. A reduction in erodibility coefficients may occur over time due to accumulation of cobbles and coarse granular material on beaches and nearshore slopes over time.

Model input parameters were entered into the GIS model for each site and the model was run to generate predicted 2006 to 2007 and 1986 to 2006 bank recession distances. Predicted recession distances were then compared to bank recession distances measured at the transect sites for the 2006 to 2007 period.

6A.3.3 Model Validation Results

Air photo measured bank recession distances obtained from 1986 to 2006 air photos and surveyed bank recession distances from 2006 to 2007 indicate that historical bank recession rates along a give shoreline segment are highly variable. Erosion transects show differences of 0 m to 3 m recession on transects located 15 m apart. Also, it is not unusual for bank recession distances to vary from up to 5 m to 10 m in local areas over the 20 year measurement period. Accuracy of field surveys is approximately +/-15 cm. Accuracy of air photo measurements is approximately +/-7 m.

Model validation results indicate that model predictions agree well with surveyed one-year bank recession distances and 20-year historical air photo measured recession distances. For the 2006 to 2007 data set, the predicted recession distance is within the measured range for four of ten comparisons, while predictions slightly over estimated recession at the remaining six sites. The average difference between model predicted bank recession and measured 2006 to 2007 bank recession is 0.3 m.

For the 1986 to 2006 data set, predicted recession distances are within the error of the measured range at 13 of 14 sites, with a difference of more than 5 m over 20 years only occurring at two sites. The average difference between model-predicted bank recession and measured 1986 to 2006 bank recession is 3.0 m.

If anything, the model tends to over-predict bank recession distances as compared to survey and air photo measurements. This may reflect a tendency toward selecting slightly conservative values for input parameters, in addition to the likelihood that erodibility coefficients used in the model are higher than erodibility coefficients for shore zone materials present at the model validation sites. To test this, erodibility coefficients used for model validation were reduced by 25% to 50%. This reduction in erodibility coefficients reduces the difference between model predictions and air photo measured bank recession distances at the validation sites. Moreover, this reduction in erodibility coefficient is thought to be reasonable for the types of shore zone materials present at the model validation sites (coarse gravel and cobble beaches adjacent to erodible banks) as compared to the type of shore zone material that will be present around the newly created Keeyask forebay shoreline (dominantly clay beaches before gravel and cobble beach deposits have time to accumulate). Erodibility coefficients typically vary by an order of magnitude for major differences in material types. Therefore, a difference of 25% to 50% seems reasonable for differences in erodibility for shore zone material types at model validation sites as compared to shore zone materials that will be present in the proposed Keeyask forebay.

6A.3.4 Mineral Erosion Model Sensitivity Analyses

6A.3.4.1 Parameters Used for Sensitivity Analyses

Sensitivity analyses have been carried out to evaluate the impact of the potential variability in key model input parameters on projected future erosion rates with the Keeyask GS in place. In undertaking sensitivity analyses, the upper bound of the 95th percentile confidence limit for two key parameters was used to test the potential upper limit of eroded mineral sediment volume, bank recession rates and bank recession distances for various modelling scenarios. These parameters are: 1) erodibility coefficient, and 2) wave energy (and corresponding maximum wave height).

6A.3.4.2 Erodibility Coefficients for Shore Materials

Erodibility coefficients for coarse- and fine textured mineral soils are based on data from calibration sites in Stephens Lake. Average erodibility coefficient values for both material types and upper and lower bounds based on a 95% confidence interval are listed in Table 6A.1-3. Average values were used for the most-likely scenario modelling. The upper bound of the 95% confidence limit has been used for sensitivity analyses. These values are as follows:

- Coarse textured mineral soil: Average: 0.00304 $m^3/J/m^2$.
- 95th percentile: 0.00361 $m^3/J/m^2$.
- Fine textured mineral soil: Average: 0.00095 $m^3/J/m^2$.
- 95th percentile: 0.00124 $m^3/J/m^2$.

6A.3.5 Wave Energy

Average annual wave energy density was calculated for the years 1971 to 2004 at 88 points around the Post-project Keeyask shoreline. These values were used to develop the wave energy input for the most likely-scenario model. For sensitivity analyses, the 95th percentile wave energy was determined at each of the 88 wave energy calculation locations and then the average ratio between the 95th percentile wave energy and the average wave energy were applied in the model. On average, the 95th percentile wave energy is 1.64 times greater than the wave energy used in the most-likely scenario model. The maximum wave height corresponding to the 95th percentile wave energy is 0.4 m, compared to 0.2 m for the most likely scenario.

Sensitivity analyses were assessed on a study area-wide basis as well as at selected test sites selected that represent a range of typical conditions in the reservoir.

6A.4 PEATLAND DISINTEGRATION AND MINERAL EROSION MODEL INTEGRATION

There are strong interactions between peatland disintegration and mineral bank erosion. Peatlands can protect mineral shores. This occurs where peatlands are located between the reservoir and mineral areas and to varying degrees where the peatlands are islands.

Mineral erosion modelling was undertaken concurrently with peatland disintegration modelling. Peatland disintegration and mineral erosion processes are highly integrated in the peatland disintegration model. A process was developed for integrating results from both models so that the resulting reservoir and shoreline polygon for all modelled time steps represents the combined effect of mineral erosion and peatland disintegration, and takes into account the interaction of these two processes temporally and spatially.

The starting point for both models is the Year 0 shoreline, that is, the shoreline that corresponds to a reservoir elevation of 159 m during 95th percentile flow conditions as predicted by Manitoba Hydro. The first modelling step conducted on peatlands entailed predicting Year 0 + 1 day and Year 0 + 60 day shorelines. Some existing floating peatlands in the flooded area whose surface are near the 159 m ASL elevation are expected to move up with reservoir filling. This is capture by the Year 0 + 1 day shoreline prediction. The Year 0 + 60 day shoreline incorporates the immediate effects of flooding on changes to nearshore peatlands and the emergence of peat islands where submerged peat is expected to float to the water's surface in the first 60 days. Both the Year 0 + 1 day and Year 0 + 60 day shorelines are segmented and classified with respect to whether the shoreline material is mineral soil or peat.

In the second modelling step, the mineral erosion model was applied to all mineral soil segments appearing on the Year 0 + 1 day shoreline, with wave energy attributes adjusted to account for the affect of peat islands that are predicted to emerge in the first 60 days after initial impoundment of the reservoir. The first modelling interval is 1 year. Predicted mineral bank recession distances in the first year were then entered into the peatland model.

In the third modelling step, the peatland disintegration model was used to predict change in reservoir area and shoreline location to the end of the first year after initial reservoir impoundment. This modelling integrated peatland disintegration processes with the mineral bank recession distances. The resulting integrated Year 1 shoreline reflects the effects of mineral erosion and peatland disintegration on the position of the shoreline during the first year.

The fourth modelling step entailed tabulating mineral and organic sediment loads for pre-defined shore zone reaches for input to sedimentation models and for environmental assessment.

This process was repeated for Years 2-5, 6-15 and 16-30 modelling periods.

The integration process included protocols for review by other members of a Peatland Disintegration Erosion Sedimentation (PD ES) working group during each modelling interval to ensure quality control.

KEEYASK
Hydropower Limited Partnership

DATA SOURCE:
Case study areas and Nelson River shoreline - ECOSTEM Ltd.; Roads - Manitoba Conservation; Water - NTS.

CREATED BY:
ECOSTEM Ltd.

COORDINATE SYSTEM:	DATE CREATED:	REVISION DATE:
UTM NAD 1983 Z15N	11-JUN-12	28-JUN-12
0 2 4 Kilometres 0 1 2 Miles	VERSION NO: 1.0	QA/QC: APPROVED

Legend

Case Study Areas

- Central Islands
- East Central
- Outside West
- West Central
- West North
- West South

- Water In 1962
- Water in 1999

Kettle Reservoir Case Study Areas

Map 6.A-1

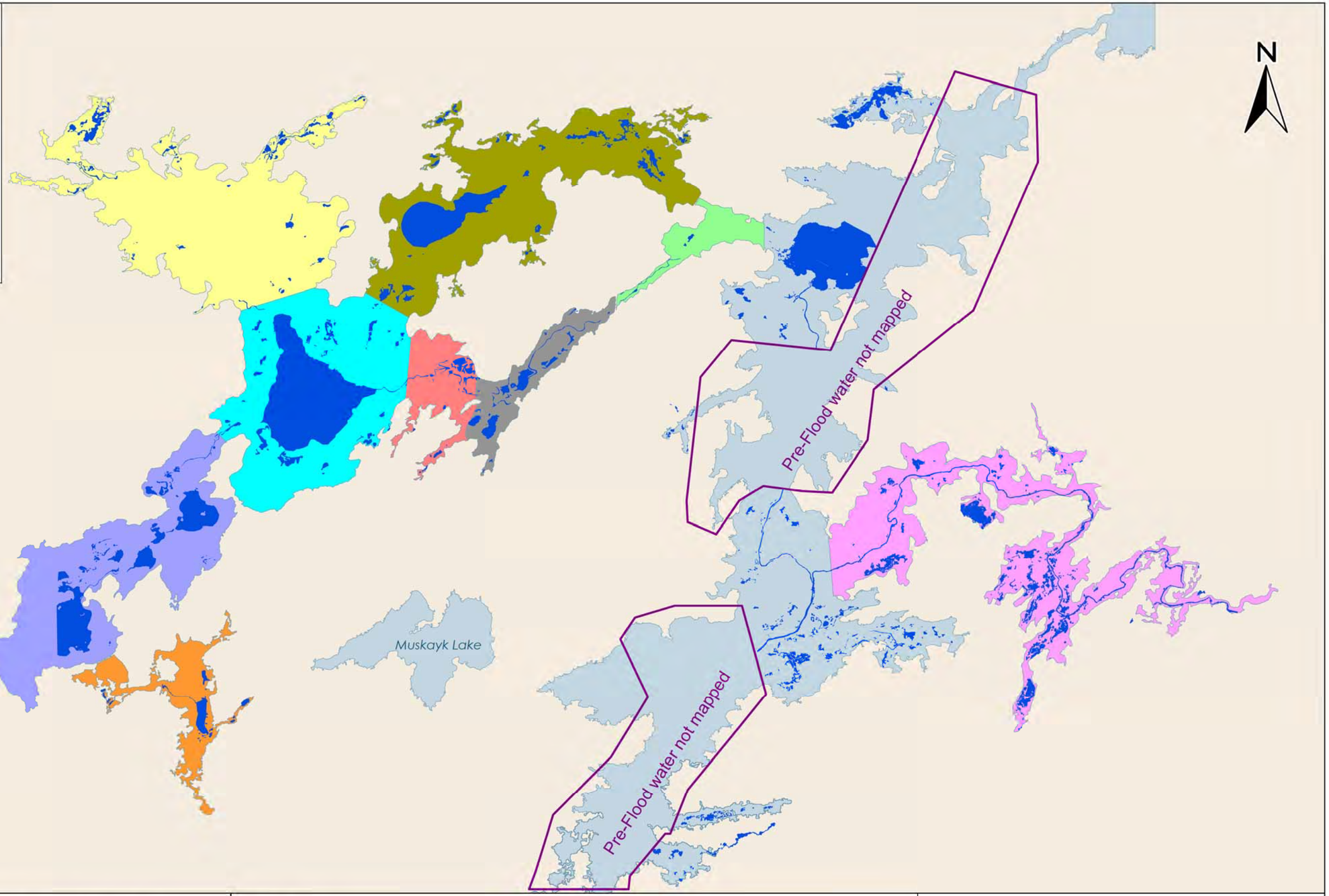

KEEYASK Hydropower Limited Partnership

DATA SOURCE:
Case study areas and water - ECOSTEM Ltd.; Roads - Manitoba Conservation; 1998 Water - NTS.

CREATED BY:
ECOSTEM Ltd.

COORDINATE SYSTEM:	DATE CREATED:	REVISION DATE:
UTM NAD 1983 Z14N	11-JUN-12	28-JUN-12
0 1 2 Kilometres / 0 0.5 1 Miles	VERSION NO: 1.0	QA/QC: APPROVED

Legend

Case Study Areas

- Central East Bay
- Channel - Main
- Channel - North
- East
- Northwest Bay
- Open Water Central
- Southeast Isolated Bay
- Southwest Bay
- Void 1978

- Water in 1969
- Water in 1998

Notigi Reservoir Case Study Areas

Map 6.A-2

APPENDIX 6B

RESULTS TABLES

This page is intentionally left blank.

6B.1 RESULTS TABLES

Table 6B.0-1: Existing Environment and Post-Project Shoreline Composition

Shoreline Length (km)						
Shoreline Type	Existing Env.	Day 1 Post-Project	Year 1 Post-Project	Year 5 Post-Project	Year 15 Post-Project	Year 30 Post-Project
Bedrock	20.8	9.8	9.7	9.7	9.9	9.7
Mineral	94.6	74.9	73.3	72.2	74.0	75.8
Mineral Overlain by Peat	25.2	0	0	26.9	76.6	91.1
Peat	64.4	167.1	183.5	145.5	73.9	54.3
Dykes and Dams	0	12.2	12.4	12.4	12.6	12.8
Total	205.0	264.0	278.8	266.7	246.9	243.6

This page is intentionally left blank.

APPENDIX 6C

PREDICTION UNCERTAINTY

This page is intentionally left blank.

6C.0 PREDICTION UNCERTAINTY

6C.1 PEATLAND DISINTEGRATION

One approach to assessing prediction uncertainty is to examine the uncertainties associated with model assumptions, inputs and parameter estimates. There is moderately high confidence in the general locations of reservoir expansion and the types of peatlands that would be affected. The general peatland disintegration patterns predicted by the model are the same as was observed at all proxy areas (see Appendix 6A for proxy area results). As well, pre-flood ecosite composition determines where peatland disintegration can occur. Ground truthing determined that ecosite mapping accuracy rates were very high for the ecosite types that highly influence peatland disintegration.

There is moderate confidence in the predicted amounts of organic sediment input. Sediment input uncertainty is an integrated uncertainty from predictions regarding maximum possible area affected, peat depth and resurfacing proportions and the timing of peatland disintegration. Confidence in the predicted maximum possible area affected is high because ground truthing of the ecosite mapping showed that mapping accuracy rates for the constraining ecosite types, mineral soil and veneer bog, were higher than 95%. Confidence in estimated peat depths is moderately high given the number and locations of soil and borehole samples in the reservoir area. There is moderate confidence in the proportion of peatland area that resurfaces during a prediction period due to limitations on available data and past research. Although confidence in surface peatland *(i.e.*, unflooded or floating resurfaced peat) disintegration rates is moderate, relatively small differences in rates would compound over time and could substantially affect later predictions. Potential for this effect should be somewhat limited given that mean annual organic sediment loads are predicted to be the highest by far in Year 1 and then rapidly decline with time.

Another approach to assessing prediction uncertainty is to compare the predicted most likely outcome to highly unlikely extreme scenarios. The predictions presented in the Shoreline Erosion section are viewed as the most likely outcomes, being based on 50th percentile values for model assumptions and parameter estimates. Peatland disintegration prediction uncertainty was further evaluated by estimating the most extreme amount of peatland disintegration in two considerably more cautious scenarios.

The non-disintegrating shoreline shows the maximum estimated maximum possible aerial extent of peatland disintegration. Based on peatland disintegration model predictions using 50th percentile model assumptions and parameters, the expected aerial extent of peatland disintegration is approximately 2.2 km^2 of peatland area during the first 30 years after flooding. Total peatland area inside the 50th percentile non-disintegrating shoreline is approximately 4.7 km^2, which is 2.2 times higher than the area that is expected to be affected by the Project during the first 30 years. Based on the very high photo-interpretation accuracy rates for the constraining ecosite types that delineate the non-disintegrating shoreline, a scenario using the 95th percentile non-disintegrating shoreline would be substantially more cautious. Total peatland area inside the 95th percentile non-disintegrating shoreline polygon area is estimated to be slightly less than 2.5 times the predicted most likely value for Year 30.

The above uncertainty levels do not incorporate the effects of future changes in background conditions or driving factors. In other words, it is assumed that the future will be the same as the past. The effects of climate change are addressed in Section 11 of the PE SV.

6C.2 MINERAL EROSION

6C.2.1 Upstream

There is moderately high confidence that the mineral erosion model captures the main parameters affecting future erosion rates and that model predicts a reliable estimate of the distribution of eroding mineral shorelines, overall extent of erosion and long term rates for modelled conditions.

There is moderate confidence with respect to the timing of change and site-specific localized erosion due to highly variable nature of the erosion process, as indicated by field survey and air photo measurements of past erosion rates.

Model validation indicated a good correlation between short term and long term historical bank recession rates and model predicted recession distance, albeit with a tendency for the model to over-predict future erosion rates by a small margin. Comparative site specific and parameter specific analyses using an independent erosion prediction model yielded similar results, confirming that the modelling approach used for the Keeyask study and results obtained are consistent with current understanding of shore erosion processes and modelling technology.

A review of with and without project flow velocities confirmed that the wave-based erosion model is appropriate for the majority of the post-project shoreline. One exception is the reach upstream of Birthday Rapids, which will see relatively little change in flow conditions with the Project, resulting in continued flow dominated erosion after the Project is in place. However, much of the shoreline in this reach is bedrock controlled with no erosion predicted by the wave model, consistent with historical erosion rates in this area. Elsewhere in this reach, the erosion model predicted low erosion rates owing to short fetches and low wave energy. Low predicted erosion rates are similar to historical rates. As a result, application of the wave model in this reach produces does not introduce significant errors in overall erosion estimates.

Mineral erosion model predictions for base loaded and peaking modes of operation indicate that the maximum erosion rates will occur during the first 5 years after impoundment, after which rates gradually decline to a significantly lower long term levels. Sensitivity analyses have been conducted to determine the impact of possible variability in erodibility coefficients and wave energy levels as compared to what were used for most likely scenario modelling.

The sensitivity analyses were done by running the model for the 95th percentile value for erodibility coefficient and wave energy while holding the other parameters at the most-likely values. Model outputs determined for each sensitivity run were: 1) system-wide yearly mineral erosion volume; 2) average top of bank recession of mineral banks; and 3) total land area lost to mineral erosion. Results from the four sensitivity runs are compared to the most-likely base case to determine potential impacts.

Table 6C.1-1 lists the results of study area wide sensitivity analyses, showing the erosion predicted for 95th percentile values as a percentage of the erosion predicted for the most-likely scenario values. During the first 5 years after initial impoundment *(i.e.*, the period considered for study area wide sensitivity analysis) peat disintegration does not affect mineral erosion rates. Therefore, results presented in Table 6C.1-1 are not affected by peat disintegration during this period. After Year 5, when peat disintegration begins to expose additional mineral shores to wave erosion the range of percentage change shown in Table 6C.1-1 is expected to continue to apply. That is, the peatland disintegration process should not affect the relative influence of the parameters considered in the system wide sensitivity analysis that was carried out.

Table 6C.1-1: Results of Study Area Wide Mineral Erosion Sensitivity Analysis

Sensitivity Parameter	% Change Over Most-Likely Base Case (Base Loaded Mode of Operation)					
	Volume Eroded		Average Bank Recession		Land Area Eroded	
	Yr 0-1	Yr 0-5	Yr 0-1	Yr 0-5	Yr 0-1	Yr 0-5
95th Percentile Erodibility Coefficient	19	14	13	9	13	9
95th Percentile Wave Energy	42	30	28	19	27	19

Model sensitivity runs were also undertaken at four test sites to assess the impact of variations of erodibility coefficient and wave energy at sites located in high, average and low wave energy environments and at sites with high and average nearshore slopes. All four test sites are located in coarse-textured mineral soil, which represents approximately 96% of the mineral banks in the first 5 years following impoundment. These analyses produced results that are similar to those obtained for study area wide sensitivity analyses. An increase in erodibility coefficient resulted in a 11% to 19% increase in annual volume eroded, a 8% to 14% increase in top of bank recession and an 11% to 14% increase in land area lost. An increase in wave energy resulted in a 25% to 44% increase in annual volume eroded, a 17% to 29% increase in top of bank recession and an 18% to 33% increase in land area lost.

6C.2.2 Downstream

There is a high level of confidence that erosion rates downstream of the generating station will be lower after the Project because there is a high certainty that the Project will eliminate ice dam formation below Gull Rapids. This in turn will eliminate the most significant factor causing shore erosion in this area.

This page is intentionally left blank.

APPENDIX 6D

DETAILED TABLES OF PREDICTED SHORELINE RECESSION AND EROSION VOLUMES

This page is intentionally left blank.

6D.0 DETAILED TABLES OF PREDICTED SHORELINE RECESSION AND EROSION VOLUMES

Table 6D.0-1: Completion of Total Project Bank Recession Distance With and Without the Keeyask Project Over the 30-Year Modelling Period[1]

	Percentage Shoreline Length – With Project Base Loaded Mode of Operation									
	Reach 1	Reach 2	Reach 3	Reach 4	Reach 5	Reach 6	Reach 7	Reach 8	Reach 9	All Reaches
Non-Mineral Banks	n/a	82.9%	3.2%	4.7%	30.8%	44.2%	52.6%	60.1%	82.7%	40.3%
0-7.5 m	n/a	17.1%	96.8%	50.8%	39.3%	34.2%	1.4%	23.4%	1.3%	37.0%
7.5-15 m	n/a	0.0%	0.0%	44.5%	28.8%	14.0%	15.6%	13.2%	9.1%	4.3%
15-22.5 m	n/a	0.0%	0.0%	0.0%	1.2%	4.3%	27.0%	3.2%	9.1%	4.3%
22.5-30 m	n/a	0.0%	0.0%	0.0%	0.0%	1.9%	1.7%	0.0%	0.0%	0.9%
>30 m	n/a	0.0%	0.05	0.0%	0.0%	1.5%	1.6%	0.0%	0.0%	0.7%
Totals	n/a	100.0%	100.0%	100.0%	100.0%	100.0%	100.0%	100.0%	100.0%	100.0%

	Percentage Shoreline Length – With Project, Peaking Mode of Operation									
	Reach 1	Reach 2	Reach 3	Reach 4	Reach 5	Reach 6	Reach 7	Reach 8	Reach 9	All Reaches
Non-Mineral Banks	n/a	82.5%	11.0%	4.1%	29.6%	38.1%	56.2%	46.6%	80.3%	47.0%
0-7.5 m	n/a	17.5%	89.0%	76.7%	49.5%	45.4%	5.2%	38.7%	2.1%	38.1%
7.5-15 m	n/a	0.0%	0.0%	19.2%	19.5%	11.2%	33.5%	14.8%	17.6%	12.5%
15-22.5 m	n/a	0.0%	0.0%	0.0%	1.4%	4.9%	5.1%	0.0%	0.0%	2.2%
22.5-30 m	n/a	0.0%	0.0%	0.0%	0.0%	0.4%	0.0%	0.0%	0.0%	0.1%
>30 m	n/a	0.0%	0.0%	0.0%	0.0%	0.0%	0.0%	0.0%	0.0%	0.1%
Totals	n/a	100.0%	100.0%	100.0%	100.0%	100.0%	100.0%	100.0%	100.0%	100.0%

	Percentage Shoreline Length – With Project, Peaking Mode of Operation									
	Reach 1	Reach 2	Reach 3	Reach 4	Reach 5	Reach 6	Reach 7	Reach 8	Reach 9	All Reaches
Non-Mineral Banks	n/a	79.6%	41.7%	11.8%	29.8%	41.9%	27.2%	60.1%	31.2%	30.9%

0-7.5 m	n/a	19.0%	54.9%	74.2%	66.4%	47.2%	61.8%	35.9%	34.7%	57.9%
7.5-15 m	n/a	1.3%	2.8%	11.3%	3.2%	7.4%	8.3%	3.0%	14.7%	7.2%
15-22.5 m	n/a	0.1%	0.6%	2.2%	0.6%	2.5%	1.9%	0.9%	3.0%	2.0%
22.5-30 m	n/a	0.0%	0.0%	0.5%	0.0%	0.6%	0.2%	0.1%	8.4%	0.5%
>30 m	n/a	0.0%	0.0%	0.0%	0.0%	0.5%	0.7%	0.0%	0.0%	1.5%
Totals	n/a	100.0%	100.0%	100.0%	100.0%	100.0%	100.0%	100.0%	100.0%	100.0%

[1]Note: Total Bank Recession Distance without the Keeyask Project can be found in maps 6.3-3 and 6.3-4; Total Bank Recession Distance with the Keeyask Project (Base Loaded mode-of-operation) can be found in maps 6.4-6 and 6.4-7.

Table 6D.0-2: Predicted Mineral Sediment Load With the Project, Base Loaded Mode of Operation

Research Reach	Total Mineral Sediment Load Due to Shore Erosion With the Project for Years After the Proposed In-Service Date											
	Yr 0-1			Yr 2-5			Yr 6-15			Yr 16-30		
	m^3	Tonnes	FT/CT*	m^3	Tonnes	FT/CT*	m^3	Tonnes	FT/CT*	m^3	Tonnes	FT/CT*
2	2.030	4,040	0/100	6,507	12,948	0/100	10,924	21,739	0/100	10,864	21,619	0/100
3	5,320	10,571	2.9/97.1	16,064	51,373	3.0/97.0	20,591	40,827	7.3/92.7	28,123	55,789	63./93.7
4	29,794	59,241	1.6/98.4	58,270	115,806	2.6/97.4	77,352	153,696	3.0/97.0	68,568	136,234	3.2/96.8
5	59,420	117,932	5.3/94.7	101,874	202,013	7.0/93.0	144,764	287,034	7.2/92.8	135,751	269,126	7.5/92.5
6	142,179	282,593	2.4/97.6	182,555	362,330	5.2/94.8	355,649	706,123	4.6/95.4	678,500	1,346,210	5.9/94.1
7	28,894	57,499	0/100	40,356	102,520	0/100	73,750	146,762	0/100	111,262	221,411	0/100
8	20,518	40,831	0/100	40,962	81,513	0/100	63,952	127,229	0.6/99.4	122,185	242,914	1.9/98.1
9	10,565	21,025	0/100	13,731	27,325	0/100	29,961	59,623	0/100	55,903	111,238	0.2/99.8
Totals	298,720	593,732	2.4/97.6	460,319	914,162	4.1/95.9	776,943	1,543,033	4.0/96.0	1,211,541	2,404,541	4.7/95.3
Average Annual Rates	298,720	593,732		115,080	228,540		77,694	154,303		80,769	160,303	

* Represents the percentage of the sediment load derived from fine-textured materials (FT) versus the percentage of the sediment load derived from coarse textured materials (CT). FT materials are predominantly silt and clay. CT materials include clay and silt with varying percentages of sand, gravel and cobbles. The number preceding the slash mark represents the fine-textured percentage, while the number following the slash mark is the coarse-textured percentage. Percentages in the totals row represent percentages across all reservoir reaches combined.

Table 6D.0-3: Predicted Mineral Sediment Load With the Project, Peaking Mode of Operation

Research Reach	Total Mineral Sediment Load Due to Shore Erosion With the Project for Years After the Proposed In-Service Date											
	Yr 0-1			Yr 2-5			Yr 6-15			Yr 16-30		
	m^3	Tonnes	FT/CT*	m^3	Tonnes	FT/CT*	m^3	Tonnes	FT/CT*	m^3	Tonnes	FT/CT*
2	1,510	3,005	0/100	4,950	9,861	0/100	8,747	17,406	0/100	8,677	17,268	0/100
3	4,171	8,282	4.5/95.5	12,575	24,985	3.1/96.9	22,924	45,526	4.0/96.0	22,418	44,473	6.2/93.8
4	20,552	40,61	1.8/98.2	44,881	89,183	2.7/97.3	61,515	122,216	3.2/96.8	28,731	102,851	5.1/94.6
5	39,602	76,602	5.2/94.8	77,473	153,634	6.9/93.1	88,929	176,158	9.1/90.9	104,690	207,548	7.5/92.5
6	70,070	139,234	2.9/97.1	109,624	217,535	5.6/9.4	176,852	350,788	6.5/93.5	342,907	679,911	7.2/92.5
7	16,543	32,921	0/100	32,671	65,016	0/100	46,263	92,063	0/100	18,510	96,349	0/100
8	12,477	24,829	0/100	30,329	60,353	0/100	47,554	94,602	0/100	74,566	148,186	2.7/97.3
9	5,858	11,657	0/100	9,230	18,368	0/100	13,788	27,439	0/100	32,361	64,393	0.2/99.8
Totals	170,783	339,391	2.7/97.3	321,738	638,946	4.1/95.9	466,572	926,198	4.9/95.1	632,860	1,255,619	5.9/94.1
Average Annual Rates	170,783	339,391		80,435	159,737		46,657	92,620		42,191	83,708	

* Represents the percentage of the sediment load derived from fine-textured materials (FT) versus the percentage of the sediment load derived from coarse textured materials (CT). FT materials are predominantly silt and clay. CT materials are clay, silt, gravel and cobbles. The number preceding the slash mark represents the fine-textured percentage, while the number following the slash mark is the coarse-textured percentage. Percentages in the totals row represent percentages across all reservoir reaches combined.